

Mestrado Integrado em Medicina Dentária
Faculdade de Medicina da Universidade de Coimbra



FACULDADE DE MEDICINA
UNIVERSIDADE D
COIMBRA

**Micromovements and Strains in Immediate Loaded
Implants:
An Ex Vivo Pilot Study**

Maria Inês da Pena de Oliveira Pereira da Silva

Orientador: Prof. Doutor Pedro Miguel Gomes Nicolau

Coorientador: Prof. Doutora Ana Lúcia de Pereira Neves Messias

Coimbra, julho 2021

Faculdade de Medicina da Universidade de Coimbra
Mestrado Integrado em Medicina Dentária

Micromovements and Strains in Immediate Loaded Implants: An Ex Vivo Pilot Study

Pereira da Silva MI¹, Messias A², Nicolau P³

¹Aluna de Mestrado Integrado, Área de Medicina Dentária, Faculdade de Medicina, Universidade de Coimbra

²Professora Auxiliar do Mestrado Integrado em Medicina Dentária, Faculdade de Medicina, Universidade de Coimbra

³Professor Associado de Prostodontia do Mestrado Integrado em Medicina Dentária, Faculdade de Medicina, Universidade de Coimbra

Área de Medicina Dentária

Faculdade de Medicina da Universidade de Coimbra

Av. Bissaya Barreto, Bloco de Celas

3000-075 Coimbra, Portugal

Tel +351 239 249 151/2

Fax +351 239 402 910

E-mail: m.inesilva.98@gmail.com

INDEX

Resumo	2
Abstract	3
List of tables	4
List of figures.....	4
Abbreviations	5
1. Introduction.....	6
1.1. Osseointegration.....	6
1.1.1.Importance of Primary Stability	6
1.1.2.Micromotions.....	7
1.1.3.Biomechanical factors that compromise osseointegration	7
1.2. Evaluation methods for primary stability.....	8
1.2.1.Insertion Torque.....	9
1.2.2.Radiographs	9
1.2.3.OSSTELL/Resonance Frequency Analysis (RFA)/Implant Stability Quotient (ISQ).....	9
1.2.4.Reverse/Remove Torque Test (Rtt).....	10
1.2.5.Periotestt®.....	10
1.2.6.Digital Image Correlation (DIC)	11
1.3. Clinical Relevance.....	11
2. Materials and methods	12
2.1. Outcome and outcome Measures	13
i. Resonance Frequency Analysis (RFA)	13
ii. Digital Image Correlation	14
3. Results.....	16
4. Discussion	18
4.1. ISQ	19
4.2. Displacement.....	20
4.3. Deformation	20
5. Conclusion	22
6. Acknowledgments.....	23
7. References	24
8. Appendices	29

RESUMO

Objetivo: A realização de carga imediata sobre os implantes está associada a maior satisfação dos pacientes uma vez que há restabelecimento da função e da estética logo após a instalação cirúrgica do implante. As cargas decorrentes da restauração imediata de implantes podem gerar micromovimentos e perda de estabilidade primária que, conseqüentemente, poderão condicionar a osteointegração e o sucesso a médio e longo prazo do implante. Este trabalho tem por objetivo avaliar o impacto da carga imediata (ciclos de carga) na estabilidade e micromovimentos de implantes de diferentes comprimentos inseridos em costelas de boi, medidos por análise de frequência de ressonância (RFA) e por correlação de imagem digital (DIC).

Materiais e métodos: Estudo experimental ex-vivo de acordo com as normas internacionais (UNI EN ISO 14801: 2016) em costelas bovinas através da colocação de 2 implantes endósseos Ø4,3 L9 mm e Ø4,3 L13 mm (CAMLOG® SCREW-LINE ConeLog® Promote® plus, (Camlog Biotechnologies®, Wimsheim, Germany). Foram exercidos sobre estes 54.000 ciclos de carga contínua variável entre 7 e 70 N. Imediatamente antes e após os ciclos de carga, foram registados os micromovimentos do conjunto pilar-implante sob carga estática crescente até 200N através do método de correlação de imagem digital (Vic-3D 2010, Correlated Solutions, MA, USA) e do quociente de estabilidade do implante (ISQ) por RFA (Osstell® ISQ IntegrationDiagnostic, Sweden).

Resultados: Não houve variação dos valores de deslocamento do conjunto pilar-implante de 13mm ao longo dos ciclos de carga. O conjunto pilar-implante de 9 mm apresentou um ligeiro aumento do deslocamento com o aumento dos ciclos de carga, todavia comparável com o conjunto pilar-implante de 13 mm. Após os ciclos e sob uma carga de 200N, foi registado um maior deslocamento lateral/horizontal (U) e vertical (V) no conjunto pilar-implante de 9mm ($165.22 \pm 51.58\mu\text{m}$ vs $121.08 \pm 37.07\mu\text{m}$ e $-84.95 \pm 25.00\mu\text{m}$ vs $-78.23 \pm 17.19\mu\text{m}$, respetivamente). Em nenhum dos implantes se registaram variações no valor de ISQ.

Conclusões: Dentro das limitações deste estudo é possível concluir que o método desenhado conforme as normas ISO 14801, juntamente com a costela bovina, conseguiram simular o comportamento de implantes em condições clinicamente semelhantes. Não foi possível antecipar qualquer variação significativa da estabilidade primária, medida como micromovimentos e ISQ, de implantes standard mais curtos face a implantes mais compridos quando expostos às mesmas condições.

Palavras-chave: Implante de carga imediata; Micromovimentos; Costela bovina; Correlação de Imagem Digital 3D (CID 3D); Análise de Frequência de Ressonância (AFR)

ABSTRACT

Trial design/objective: Immediately loaded implants are associated with greater patient satisfaction since function and aesthetics are re-established immediately after surgical installation. The recurrent loads on the immediate restoration of implants can cause micromovements and loss of primary stability that, consequently, may condition the osteointegration process and, in the short/medium term, the success of the implant. This experimental work aims to evaluate the impact of immediate loading (load cycles) on the stability and micromovements of different length implants inserted in bovine ribs, measured by resonance frequency analysis (RFA) and digital image correlation (DIC).

Methods: An ex vivo experimental study according to the international standards (UNI EN ISO 14801: 2016) in bovine fresh ribs placing 2 endosseous $\varnothing 4,3$ L9 mm e $\varnothing 4,3$ L13 mm (CAMLOG® SCREW-LINE ConeLog® Promote® plus, (Camlog Biotechnologies®, Wimsheim, Germany). Exerted on these were 54000 cycles of a varying load between 7 and 70. Immediately before and after the loading cycle, the micromovements from the implant-pilar complex were registered under a rising static load until 200N through the image correlation method (Vic-3D 2010, Correlated Solutions, MA, USA) and the Implant Stability Quotient (ISQ) was registered by RFA (Osstell® ISQ IntegrationDiagnostic, Sweden).

Results: Both implants' values increased similarly after the loading cycle. The displacement was slightly higher and constant in the 13 mm implant. At 200 N, the components V, U and Von Mises strains presented higher discrepancy in the 9 mm implant. After the cycles and under a 200N load, a higher displacement lateral/horizontal (U) and vertical (V) in the abutment-implant complex in the 9mm ($165.22 \pm 51.58\mu\text{m}$ vs $121.08 \pm 37.07\mu\text{m}$ e $-84.95 \pm 25.00\mu\text{m}$ vs $-78.23 \pm 17.19\mu\text{m}$, respectively). Neither implant registered varying ISQ values.

Conclusions: Within the limitations of this study, it is possible to conclude that the method developed following the ISO 14801 norms together with the use of a bovine rib can simulate the implant performance in clinical conditions. The conjoint use of digital image correlation and RFA to assess strains, displacement and ISQ values are essential to evaluate the implant stability. It is not possible to anticipate any significative variation for the primary stability, measured as micromovements and ISQ, of shorter standard implants compared to longer implants when exposed to the same conditions.

Keywords: Immediate loading implant; Micromovements; Bovine ribs; 3D Digital Image Correlation (3D DIC); Resonance Frequency Analysis (RFA)

LIST OF TABLES

Table 1 – ISQ values obtained before and after loading cycles.

Table 2 – Peak, minimum and mean \pm SD displacements (μm) in the lateral/horizontal (U) and vertical (V) directions; Peak values of the principal maximum strains (e1), principal minimum strains (e2) and Von Mises strains (μe) at 200N.

LIST OF FIGURES

Figure 1 – Loading set up (a) with the stereo cameras assembled (b).

Figure 2 – Representation of the loading period according to ISO 14801:201630 regulation.

Figure 3 – Uniaxial compression test data the two implants.

Figure 4 –Two-dimensional representation of 9 mm implant before and after the loading period of the U component (a.1; a.2), V component (c.1; c.2) and Von Mises strains (e.1; e.2), as well as the 13 mm implant with the U component (b.1; b.2), V component (d.1; d.2) and Von Mises strains (f.1; f.2).

ABBREVIATIONS

∅:	Diameter
μe:	Microstrain
μm:	Micrometers
2D:	Two-Dimensional
3D:	Three-Dimensional
AMD:	Área de Medicina Dentária
BIC:	Bone-Implant Contact
CAD_CAM:	Computer Aided Design – Computer Aided Manufacturing
CBCT:	Cone Beam Computer Tomography
DEM:	Departamento de Engenharia Mecânica
DIC:	Digital Image Correlation
FCTUC:	Faculdade de Ciências e Tecnologia da Universidade de Coimbra
FEA:	Finite Element Analysis
FMUC:	Faculdade de Medicina da Universidade de Coimbra
HU:	Hounsfield Unit
IMM:	Implant Micromotions
ISEC:	Instituto Superior de Engenharia de Coimbra
ISO:	International Standardization Organization
ISQ:	Implant Stability Quotient
L:	Length
MM:	Micromotions
PTV:	Periotestt Value
QEI:	Quociente de Estabilidade do Implante
RFA:	Resonance Frequency Analysis
RTT:	Reverse/Remove Torque Test

1. Introduction

The loss of one or more teeth can negatively affect a person's oral health, with the patient's appearance being the most problematic consequence and the primary reason for seeking prosthodontic treatment¹.

There are three basic approaches to a partial or complete edentulous patient including removable dental prosthesis, fixed dental prosthesis and dental implants¹. The placement of dental implants for oral rehabilitation is a therapeutic option increasingly studied and used. It aims to restore masticatory, phonetic, and aesthetic functions in patients.

1.1. Osseointegration

1.1.1. Importance of Primary Stability

The term osseointegration, defined by Branemark et al², describes a direct connection between implants and living bone without the formation of a fibrous tissue encapsulation when subjected to excessive masticatory functional loads.

Osseointegration is also a measure of implant stability, which will occur if a primary and secondary stage of implant stability is achieved.

Primary stability of an implant mostly comes from an immediate mechanical adaptation and engagement with the cortical bone. This mechanical stability is defined as its ability to sustain cyclic loading without producing excessive damage in the bone and micromotions at the interface. However, as suggested in the literature, there is a critical threshold of micromotion above which fibrous encapsulation prevails over osseointegration³⁻⁵.

Secondary stability offers biological stability through bone regeneration and remodelling, having new bone-forming at the implant surface⁶. While primary stability is a prerequisite for secondary stability to work, the latter determines the timing for functional loading⁴.

During osseous healing, implant stability decreases until secondary biologic stability is established⁷. At approximately four weeks after implant placement, secondary stability starts to increase. At this time point, the lowest stability is expected. Therefore, to achieve adequate stability before occlusal loading, the classic Brånemark² protocol proposes a 3-to-6-month non-loaded healing period in the maxilla and 3-to-4 months in the mandible^{4,5}.

However, updated protocols have shortened the healing period, making it possible to load implants earlier and even immediately, before osseointegration is completely obtained⁵. Immediately loaded implants have shown long-term predictability, similar to conventionally

loaded implants when osseointegration is complete⁸. Rehabilitation time decreases with immediate loading, increasing patient satisfaction and reducing delays for the final restoration⁸.

1.1.2. Micromotions

The absence of movement immediately after implant insertion is one of the most important factors regarding implant osseointegration⁹. Implant micromotion (IMM) during the healing phase is known to be one of the main causes of implant failure^{10,11}. IMM is the movement or displacement between bone and implant upon application of occlusal forces. Excessive IMM at the bone-implant border has been shown to have a negative influence on osseointegration and bone remodelling⁹⁻¹¹.

The micromotion threshold above which there is risk of formation of a fibrous connective tissue at the bone-implant interface¹² is reported to be between 50 and 150 μm . IMM is dependent on factors such as the implant design, implant-abutment connection, quality and density of the bone, occlusal load, existing parafunction, restorative material, and the morphology of the occlusal table¹³.

1.1.3. Biomechanical factors that compromise osseointegration

As previously mentioned, in early and immediate loading protocols, primary implant stability is one of the most important factors in achieving predictable treatment¹⁴. There are factors, either individual, such as bone quality, or treatment-related such as implant geometry and surgical procedure, that influence the primary stability¹⁵.

Bone Quality and Density

Mechanical properties of the bone are an important factor in osseointegration. To achieve the necessary torque value to perform immediate loading, it is important to evaluate the bone density at the implant site⁵.

Several classifications regarding bone density have been proposed. One of the most popular classification was elaborated by Lekholm and Zarb¹⁶, in 1985, and then modified by Mish¹⁷ in 1990. This classification is based on bone macroscopic morphology and distribution of cortical and trabecular bone, determining their quality and density⁵. We can then say that there are four bone types ranging from type I with more dense cortical bone, to type IV, with thin cortical bone and low trabecular density⁵.

Surgical principles of implant dentistry state that primary stability, as well as adequate blood flow, are required to ensure that the local metabolism is not disrupted, and that healing is facilitated resulting in osteointegration of the dental implant⁵.

Bone types I and IV are not good candidates for implant placement. Despite being ideal for primary stability, type I bone presents very thick and dense cortical bone that impairs the required blood flow for the healing process. On the contrary, type IV bone presents a very thin layer of cortical bone which is disadvantageous to achieve the desired primary stability, even though blood flow is abundant for the successive stages of healing^{5,17}. Notwithstanding this, the operator can overcome the limitations associated with type IV bone by performing specific surgical techniques and choosing implants with especial macro designs⁵.

Implant geometry

The configuration of an implant is considered an essential requirement for implant success¹⁸. Implant geometry can be divided into macro and micro geometry.

The macrogeometry refers to implant morphology including size, design, length, diameter, kind of surface or distance between threads^{19,20}.

Regarding implant length, longer implants are mostly preferred, with a minimum of 8 mm length, being 13 and 15 mm implants the most frequently used⁵. Nevertheless, implant adaptation to the existing bone anatomy is a far more suitable alternative. The use of short implants expands treatment options and reduces the need for significant bone augmentation procedures in cases with diminished bone height in edentulous areas²¹. In fact, it has been demonstrated that implant diameter has a greater influence on stress and strain than implant length²¹.

Microgeometry is distinguished for surface treatments that, according to literature, can vary between etching, sandblasting, and anodizing the surface. However, all share the same purpose, to increase rugosity, making the area of implant-bone contact even more extended^{5,19}.

1.2. Evaluation methods for primary stability

Being able to quantify implant stability at various time points and to project a long-term prognosis based upon measured implant stability is of an utmost importance⁴. Presently, there are various diagnostic analyses suggested to define implant stability as shown below.

1.2.1. Insertion Torque

The measurement of the moment of force (torque) necessary to insert an implant in its lodging place in the bone is a parameter for studying initial stability²².

By increasing the insertion torque, it is possible to improve an implant's primary stability. Still, stress and strain on the peri-implant bone can occur with high implant insertion torque, inducing deleterious effects on the local microcirculation, leading to bone necrosis and increasing the risk of implant failure²⁰.

To achieve good primary stability without creating excessive compression in the peri-implant bone, it has been suggested that implants should be inserted with a torque between 30 to 40 Ncm⁻¹, depending on the bone density^{14,20}.

1.2.2. Radiographs

Radiographs are a non-invasive method and can be performed at any stage of healing or function. An implant is deemed successful if presents up to 1.5 mm bone loss after the first year of loading and an additional loss of 0.1 mm/year afterwards⁴.

Usually, periapical radiographs are taken to measure the crestal bone level at the proximal sites of the implant, becoming a significant radiographic indicator of implant success. Standardization of the image acquisition is important to ensure reproducibility and accurate evaluation of marginal bone levels.

Nevertheless, neither periapical radiographs nor panoramic radiographs are capable of determining facial bone levels (buccal or palatal/lingual), where a considerable amount of bone resorption occurs. Computerized Tomography (CT) and computer-assisted measurements can provide additional information with a reported accuracy of approximately 0,1mm⁴.

1.2.3. OSSTELL/ Resonance Frequency Analysis (RFA) / ISQ

The resonance frequency analysis (RFA) is a non-invasive, contactless, subjective, and reproducible method to measure implant stability, being able to use at any time during the healing process^{20,22}.

With the RFA, a numerical value known as implant stability quotient (ISQ) is obtained, ranging from 1 to 100.

Osstell® (IntegrationDiagnostic, Sweden) is the most used device to measure RFA. This magnetic system includes a transducer (wireless smartpeg) attached to the implant or abutment. A magnet is located at the end of the transducer, and, through magnetic stimulation, the pin vibrates emitting voltage. This voltage measurement reaches the resonance frequency analyser, which reports an ISQ value. The higher the ISQ, the greater the implant anchorage to the bone, and the steadier the implant is^{20,22}.

Specialized literature describes that ISQ values ranging from 57 to 82 are usually connected to better osseointegration with an average of 69 after a year of loading. ISQ values lower than 40 involve high-risk situations for the implant, while values higher than 55 are considered favourable²⁰. However, RFA values have never been directly correlated to implant micromotion, so they must be considered approximate measurements²².

1.2.4. Reverse/Remove Torque Test

The reverse torque test (RTT), developed by Johansson and Albrektsson²³⁻²⁵ after being proposed by Roberts et al²⁶, evaluates the “critical” torque threshold where bone-implant contact (BIC) is disrupted⁴. This indirectly provides information on the degree of BIC of an implant⁴.

Removal torque depends on the implant material as well as the quality and quantity of bone. In type IV bone, for example, the RTT is generally lower than in denser bone. This, however, does not reflect the degree of osseointegration and, most importantly, cannot be used in clinical practice⁴.

1.2.5. Periotestt®

The Periotestt® device measures the damping capacity of an implant that has been tapped and deflected by the instrument's hitting pistil, during repetitive percussions (16 times) on the implant^{22,27}.

This measuring procedure is electromechanical. Contact time of the pistil onto the deflecting implant is calculated into the Periotestt value (PTV). This value, which is dependent on the implant stability, has no measurement unit and ranges from - 8 (rigid integration) to + 50 (non-integration)²⁷.

1.2.6. Digital Image Correlation (DIC)

Digital Image Correlation (DIC) is an innovative non-contact optical technique for measuring strain and displacement²⁸ on the surface of an object before and after deformation by using one (2D-DIC) or two (3D-DIC) digital cameras to capture the surface images²⁹. From one image to the next, or from the non-deformed to the deformed status, the method tracks changes in the configuration of grey speckle patterns in small squares sections of the entire image, called subsets²⁹.

1.3. Clinical relevance

One could hypothesize that with short implants it is more challenging to maintain primary stability than with longer implants when submitted to immediate loading, possibly resulting in early implant loss.

However, anatomical defects (limited height) in implant sites where immediate rehabilitation is required for functional or aesthetic reasons might limit the possibility of inserting longer implants thus restricting the clinician to the use of shorter implants (within standard length). Despite reducing the crown-implant ratio, this option dismisses additional surgical procedures to implant placement, such as bone augmentation, resulting in shorter treatment time, reduced costs and less morbidity²¹.

Thus, it is important to understand if implants with different crown-implant ratios withstand immediate load likewise, that is if smaller length implants and longer implants maintain primary stability similar after a post-insertion loading period.

2. Materials and methods

Two anatomically similar fresh bovine ribs with 4 to 5 cm length were selected and cleaned from all attached soft tissues including periosteum using a scalpel and a molt to receive **two implants** Ø4,3 L9 mm and Ø4,3 L13 mm (CAMLOG® SCREW-LINE ConeLog® Promote® plus, (Camlog Biotechnologies®, Wimsheim, Germany), one per rib.

The implant socket preparations were done by a single experienced surgeon following the standard drilling protocol recommended by the manufacturer. Initially, a punch-mark was made on the desired implant position with the Ø2.3 mm round bur at 800 rpm. Using a Ø2.0 mm pilot drill, a 6 and 10mm deep drill was made along the implant axial followed by form drillers until the TAP drill Ø4.3mm that gave the final shape. Abundant manual irrigation was used throughout the site preparation. (Appendix I)

The appropriate key for the Camlog Screw-line Implants Conveyor was selected and coupled to the handpiece. The implants were placed using a handpiece with an electric handpiece (Surgic Pro+, NSK Europe Ltd.©) with torque and speed regulated at 30 Ncm⁻¹ and 50 rpm. Final manual tightening was made using the torque control wrench up to 45 Ncm⁻¹. Each implant was positioned 3mm supracrustal, in accordance with ISO 14801:2016³⁰ regulation for fatigue testing of dental implants.

One hemispherical chromium-cobalt loading member with 4mm radius and 8mm height was milled and cemented to a Ø4.3mm, L2.0mm Conelog Titanium base CAD/CAM (Camlog Biotechnologies®, Wimsheim, Germany) using a dual curing resin cement (DuoCem®, Coltène, Altstätten, Switzerland). The abutment was tightened to the implants with 30Ncm⁻¹ to undergo dynamic loading following the indications of ISO 14801:2016³⁰.

In order to comply with the indications of ISO 14801:2016, a support was built (in collaboration with Laboratório de Biomecânica, Instituto Superior de Engenharia de Coimbra (ISEG)) to hold the ribs and place the implants with the central longitudinal axis making a 30° angle with the loading direction of the testing machine³⁰.

The complete assembly was then placed in an all-electric dynamic test instrument (INSTRON® ElectroPuls™ E10000, Norwood, MA, USA). Load was applied using a loading plate clamped to the test instrument using a rod with an intermediate joint to ensure no bending moments are applied with the axial load, as represented in Figure 1 and Appendix II.

The design followed the ISO 14801 norms, with its central longitudinal axis making a 30° angle with the loading direction of the testing machine³⁰.

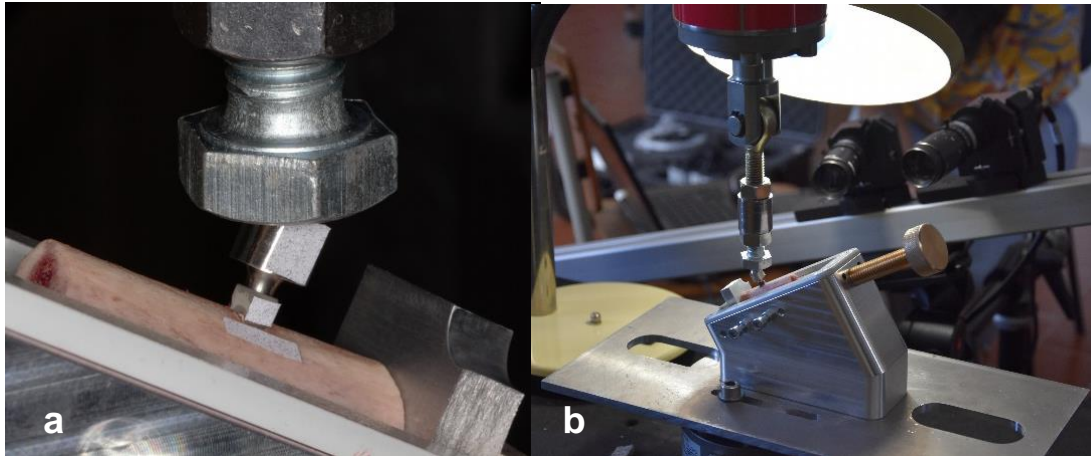


Fig. 1 – Loading set up (a) with the stereo cameras assembled (b).

This experimental study simulates the first month of functional loading of the implant, which is reflected in a number of chew episodes. According to Farooq et al³¹, the average chews per meal are 660 ± 276 with an average chewing rate of 1.44 ± 0.24 chews per second (1.44 Hz). Po et al³² also stated that the mean frequency of a chewing episode is 1.57Hz. The present study considered 3 meals per day for a 30-day period and an approximate number of 600 cycles/meal, totaling 54.000 chewing cycles. Cyclic load application ranging from 7 to 70N was used to simulate the chewing cycles. To prevent decomposition of the bovine ribs, the load application frequency was increased to 10Hz, complying with the prerequisite of ISO 14801:2016 that rules load frequency $<15\text{Hz}$ ³⁰.

The test instrument (INSTRON® ElectroPuls™ E10000, Norwood, MA, USA) was programmed to gradually increase the loading cell to the mean force value of the sinusoidal curve (38.5 N). Afterwards, load varied cyclically between a maximum of 70N and a minimum corresponding to 10% of the maximum force (7N), generating a sinusoidal load curve, as illustrated in Figure 1.

The duration of the test for each implant was, therefore, 1h30m.

Before and after each dynamic load test, the implant-abutment assembly was submitted to a quasi-static linear increasing load from 0 to 200N to register the initial and final displacements.

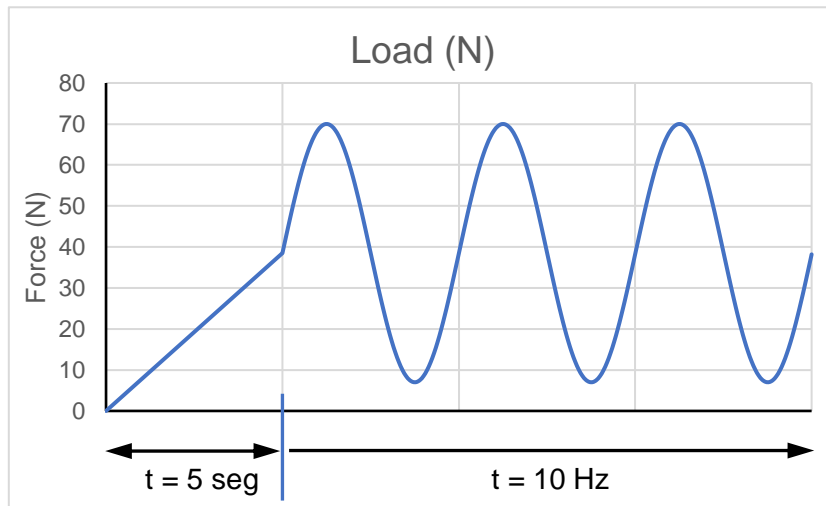


Fig. 2 – Representation of the loading period according to ISO 14801:2016³⁰ regulation.

Outcomes measures

i. Resonance Frequency analysis (RFA)

Immediately before and after loading, the ISQ was measured using an Osstell ISQ® (Osstell AB, Göteborg, Suécia) device. A suitable transducer was inserted into the implant body (Smart Peg) and measurements were done in two different directions (mesial and buccal). The tip of the instrument/device was kept perpendicular to the Smart Peg according to manufacturer guidelines.

i. Digital Image Correlation (DIC)

A random isotropic speckle pattern was obtained by spraying black ink with an airbrush on white sticker paper and applied to the hemispherical loading member and exposed portion of the implant neck.

Two stereo high-speed cameras (Point Grey GRAS-20S4M-C) were assembled following the manufacturer's instructions (Correlated Solutions®, Columbia, USA) to capture displacement of the speckle pattern at the maximum resolution of 1624x1224 pixels) and a maximum frame rate of 19 frames per second.

Both cameras were fixed to their rotating mounting devices and positioned symmetrically about the implant-abutment assembly with the stereo angle between 20° and 45°, keeping a constant magnification and providing synchronized stereo images. The specimens were positioned with the pattern of spots facing the cameras (Fig 1.)

Images captured were analyzed with Vic-3D 2012 (Correlated Solutions®, Columbia, USA), the captured real-time images were analyzed. For each specimen, the peak/maximum values of displacement were collected at 50 N, 100 N, 150 N and 200N, in the transformed U and V axes as well as the maximum, minimum and von Mises principal strains distribution over the implant neck/abutment surface (Figure 1).

The stereo system was calibrated beforehand, using a 25 mm length and 3 mm pitch 9 x 9 dot grid. The calibration reflects the capacity of the transformation algorithm to convert deformation into displacements. The calibration's final score is displayed in pixels and, the lower the value the more accurate the algorithm. Since the 13 mm implant score was 0,0083 and the 9 mm was 0,0052, it indicates that there were no systematic errors.

Since it is a pilot study and only two implants were tested, no statistical methods were employed.

3. Results

The results obtained for the ISQ values for the 9 mm implant and the 13 mm implant were assessed for determining the effect of implant length on RFA (Table 1).

These results suggested that both implants increased their ISQ after the loading cycle, showing similar values, despite the 9 mm implant being somewhat lower.

	9 MM IMPLANT		13 MM IMPLANT	
	Mesial	Buccal	Mesial	Buccal
INITIAL ISQ	74	74	76	77
FINAL ISQ	75	75	78	78

Table 1 – ISQ values obtained before and after loading cycles.

For each specimen, values of implant displacement were recorded in millimetres before and after tests were done at 50N, 100N, 150N and 200N loads, being afterwards converted into micrometers.

The two implants presented similar values of displacement. However, in Graphic 2 a slightly higher displacement is noticeable on the 13 mm implant, either at minimum or maximum.

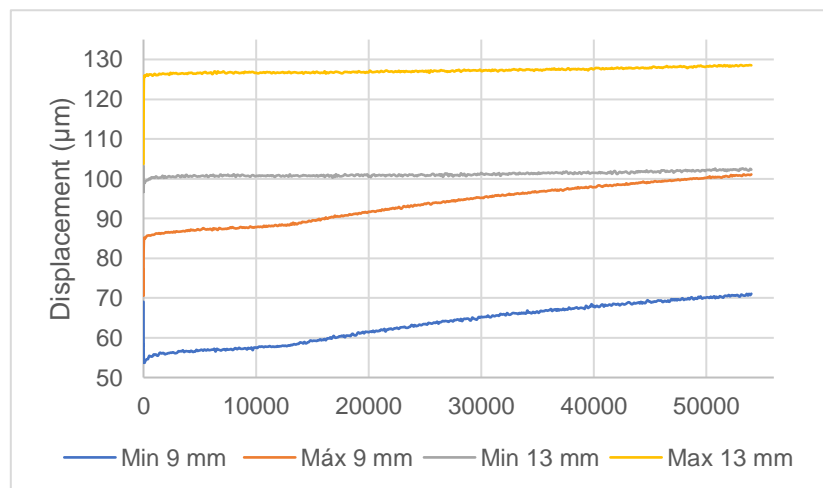


Fig. 3 – Uniaxial compression test data the two implants.

As can be seen in Figure 4, the difference from the initial and final displacement for the 13 mm implant, either lateral (U) and vertical (V), were minimal. In the 9 mm implant the displacement discrepancy seems a bit higher. These interpretations can be validated with the information in Table 2, were values of the peak and minimum displacement in V, U, and Von Mises strain for each implant at 200 N obtained using DIC.

The Von Mises strain distribution, a measure of the deformation, is also represented in Figure 4. The images after the loading period present strain accumulation on the extreme ends of the abutment, being more evident on the 9 mm implant. However, when looking at Table 2, were

values of the peak and minimum displacement in V, U, and Von Mises strain for each implant at 200 N are summarized, the difference does not seem significant.

Appendix III represents the rigidity variation of the system implant-bone along the loading period.

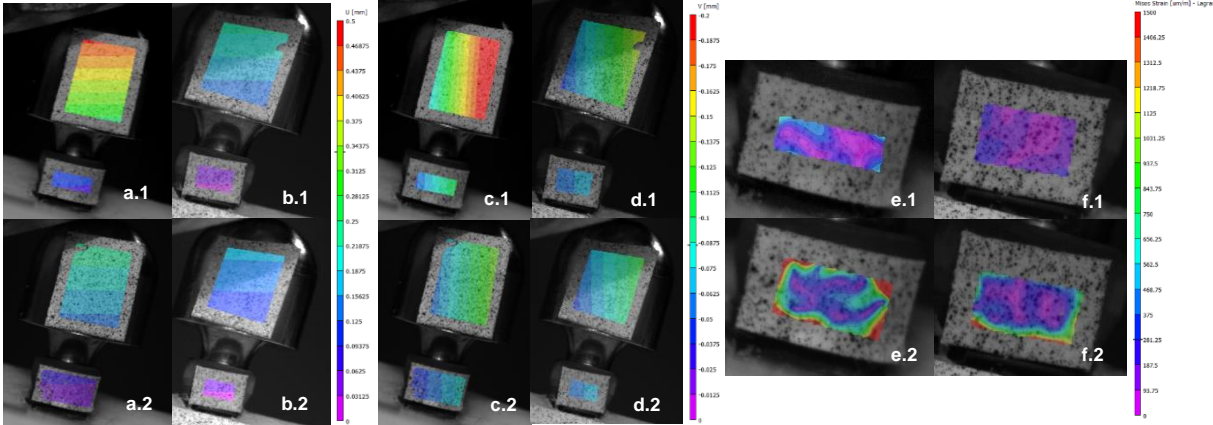


Fig. 4 – Two-dimensional representation of 9 mm implant before and after the loading period of the U component (a.1; a.2), V component (c.1; c.2) and Von Mises strains (e.1; e.2), as well as the 13 mm implant with the U component (b.1; b.2), V component (d.1; d.2) and Von Mises strains (f.1; f.2).

		200 N			
ABUTMENT	U		Peak (µm)	Minimum (µm)	Mean ± SD
		9 mm	Initial	478.06	78.20
		Final	424.15	39.80	165.22 ± 51.58
	13 mm	Initial	232.88	25.65	157.72 ± 170.07
		Final	168.28	25.62	121.08 ± 37.07
	V				
		9 mm	Initial	-236.39	-46.63
		Final	-136.05	-37.26	-84.95 ± 25.00
13 mm	Initial	-154.59	-43.18	-93.07 ± 29.94	
	Final	-117.57	-42.64	-78.23 ± 17.19	
IMPLANT	9 mm		E1 (peak, µε)	E2 (peak, µε)	Von mises (peak, µε)
		Initial	933.24	-1527.66	737.39
		Final	6206.66	-10111.7	5773.26
	13 mm	Initial	147.40	-948.11	478.94
		Final	4130.05	-1446.01	2057.80

Table 2 – Peak, minimum and mean±SD displacements (µm) in the lateral/horizontal (U) and vertical (V) directions; Peak values of the principal maximum strains (e1), principal minimum strains (e2) and Von Mises strains (µε) at 200N.

4. Discussion

In Dentistry, it has been axiom that longer implants guarantee greater primary stability by increasing bone contact, although a linear relationship between both has not yet been established³³.

Short implants are not frequently advised because occlusal forces are thought to be distributed over a large implant surface area, preventing excessive strains at the interface. The occlusal forces are distributed largely to the crestal bone, rather than equally throughout the entire surface area of the implant contact, according to a Lum LB et al study³⁴. Masticatory forces are usually well tolerated by the bone because they are light and temporary. This could explain why implant length is not proportional to biomechanical stability³⁵.

This experimental study aimed at the evaluation of the primary stability, displacements, and strains on different length implants with the aid of RFA and DIC.

Despite being one of the most extensively used procedures to check implant stability, RFA does not allow the direct analysis on the displacements of dental implants, presenting some limitations, such as: the impossibility of evaluating the stability of many implants with different lengths and widths or when inserted in different bone densities. Another drawback is that after inserting the definitive crown, this approach cannot be used when the crown is placed on the implant without removing or destroying it, which is inconvenient or impossible in some clinical scenarios³⁶. Nevertheless, in this experimental study this last issue was not a problem because only the implant abutment was used. RFA is considered by the literature a good procedure to check stability of the same implant during a period of time, and this was the case in this study for each implant^{20,27,37}.

Experimental methods such as the strain gauge³⁸, a well-documented method, and more recently DIC^{39,40}, can validate numerical stress and strain in implants and surrounding bone. DIC method uses a full-field non-contact optical technique that works on the surface of practically any material, which is more precise than traditional manual measurement methods⁴⁰.

Up to our knowledge, this is the first ex vivo study following the ISO 14801 norms³⁰ on immediately loaded implants with different lengths, measured by RFA and DIC techniques in a bovine rib.

Our study followed the same methodology as Messias et al³⁹ despite not sharing the same objective. Both were conducted according to the ISO regulation for fatigue testing of single dental implants and prosthetic components, simulating functional loading under “worst-case” conditions. A 3 mm distance between implant shoulder and the bovine rib was considered to

represent reduced bone support and load application at 30° off-axis meant to range from normal bite forces to maximum bite or parafunctional forces^{41,42}.

4.1. ISQ

Primary stability of the implant can be defined as the absence of MM immediately after insertion of the implant into the bone bed⁴³.

As mentioned before, IMM can be tolerated until 150 µm, any displacements beyond that can be considered as excessive MM. The displacement displayed in Figure 3 of both implants is under 130 µm. The 13 mm implant displayed a constant displacement value while the 9 mm was slowly increasing throughout the loading period.

Liang Kong et al¹⁸ used a nonlinear finite element method to evaluate the effects of implant length and diameter on the maximum displacement in immediate loading models. They concluded that an increase in length under an axial load decreased the maximum displacement of the implant-abutment complex.

In our study, when comparing implants of 2 lengths, the 13 mm implant had marginally higher ISQ values and displacement than the 9 mm implant, both prior and after loading, as described in Table 1 and Figure 3, respectively. However, as said above RFA does not allow the direct analysis comparing displacements of dental implants with different lengths, it can however help set a prognosis on the implant stability of the same implant (9 or 13mm) before and after loading and in this case scenario (type of bone and number of loading cycles), we can expect that both implants are suitable for immediate loading on the condition that after loading both implants had slightly higher ISQ values.

These outcomes coincide with other previously published studies⁴³⁻⁴⁵, which, although not sharing our objective, also measured implant stability by means of RFA and the impact of different lengths at implant insertion.

Degidi et al⁴⁴ results showed that the ISQ values decreased while length increased (except the 8 mm implant that had higher values than the 9,5 mm and 11 mm implant). In Barakani et al⁴³, the 13 mm implant also had higher ISQ values than the 10 mm implant in D3 bone. However, both concluded that diameter and length do not seem to influence primary stability.

Weerapong et al⁴⁵ article is one of few that compares short implants (6 mm) to standard implants (10 mm) in an immediate loading setting. They found that early loading of short implants is comparable to conventional-length implants when bone quality and primary stability are optimal.

On the other hand, the results are in contrast with other studies that reported a higher stability with increased implant length achievement of a better primary stability¹³. These contradictory results are most likely due to a lack of uniformity in the implant design, the insertion surgical protocol, and the sample size analysed.

4.2. Displacement

The images obtained with the DIC stereo system allowed the measurement of displacement on the surface in two directions, U and V, and the visualization of the deformation of each specimen (Figure 4).

After analysing the images regarding the lateral component (U) and the vertical component (V), the 13 mm implant shows an insignificant difference between initial and final displacements. Contrarily, the 9 mm implant difference is more evident. This discrepancy can also be seen in either Figure 3 or Table 2. The distribution pattern of displacement at the right side of the 9mm implant in the U component reflects a traction pattern. Meanwhile, in the V component, the higher negative value on the left side means that the implant is suffering compression.

Liang Kong et al¹⁸ article used a Nonlinear FEA to simulate realistic screw-implant connections models to examine the frictional contact between the interface jawbone-implant. One of variables studied was the maximum displacement of the implant-abutment complex in different lengths (6, 11 and 16 mm). They verified that, similarly to our results, longer implants presented lower maximum displacement¹⁸. Other study with a similar study design, also evaluated the influence of 6 mm and 10 mm implant immediately loaded in D4 bone quality and shared the same conclusion⁴⁶.

4.3. Deformation

Regarding the Von Mises strain component, both implants were exposed to some deformation, despite the measurements on the 13 mm surface being minimal before and after loading. Once more, the strain values were more noticeable on the 9 mm implant.

On the same articles mentioned above, Liang Kong et al¹⁸ and R. Desai et al⁴⁶ measured the maximum von Mises stresses under 100 N axial force. Once again, longer implants were associated with lower maximum deformation.

Unfortunately, the literature on the length impact in immediately loaded implants measured by DIC or FEA is scarce, and in most studies, short implants refer to implants <8 mm.

Even though our outcomes demonstrated that the displacement and deformation difference were higher on the 9 mm implant when compared with the 13 mm, it does not mean that shorter standard implants should not be used in an immediate loading seating. When analysing the data, values progressed to a better state, with lower values.

Since we only applied an equivalent to a month of functional load, we can only assume that shorter immediate loaded implants have similar results to longer ones during the early stage of treatment.

Since it is a qualitative study, only using two implants is an intrinsic limitation of this study. Despite the proximity of this experiment design to clinical conditions, various study design flaws may restrict the clinical implications addressed by the acquired data.

Some limitations are associated with an ex vivo experimental study such as the time limitation of having bovine ribs as an implant bed because suffers decomposition.

Further studies with larger samples sizes are required to ascertain the influence of implant length in the micromovements and strains in immediate loading implants.

5. Conclusion

Within the limitations of this experimental study, it is possible to conclude that:

- The method developed following the ISO 14801 norms together with the use of a bovine rib can simulate the implant performance in clinical conditions.
- The conjoint use of digital image correlation and RFA to assess strains, displacement and ISQ values of the length impact in micromovements are essential variables to evaluate the implant stability.
- Despite displaying some differences in the data obtained when comparing both implants, they were considered minimal.
- This is an exploratory research, with a qualitative approach and the achieved results are not to generalize but rather to provide a contextualized understanding. Nevertheless, our study indicated that both shorter standard implants ($\geq 9\text{mm}$) and longer implants ($\leq 13\text{mm}$) have similar behaviours when exposed to the same environments.

ACKNOWLEDGEMENTS

I would like to thank my supervisors Professor Doutor Pedro Miguel Gomes Nicolau for providing guidance and feedback throughout this project and Professora Doutora Ana Lúcia de Pereira Neves Messias whose dedicated support, insight and knowledge into the subject matter steered me through this research.

I am grateful to Professor Doutor José Domingos Moreira da Costa and Professora Doutora Maria Augusta Neto for their invaluable knowledge and patience during the time spent together in the lab.

My gratitude goes to Professor Doutor Fernando Guerra for his kind collaboration in the project.

To Nuno António Simão da Cruz, whose contribution was essential to this project, I am deeply thankful.

Also, I would like to thank my teachers that helped me during my academic formation and to my colleagues and friends for the unconditional support.

And my biggest thanks to my family for all the support they have shown me through five years of learning and on this research, without whom I would not have made it through.

6. References

1. Singh M, Kumar L, Anwar M, Chand P. Immediate dental implant placement with immediate loading following extraction of natural teeth. *Natl J Maxillofac Surg*. 2015 Jul-Dec;6(2):252-5. doi: 10.4103/0975-5950.183864. PMID: 27390509; PMCID: PMC4922245.
2. Brånemark, P.-I.; Zarb, G.; Albrektsson, T. (1985) *Tissue-integrated prostheses: osseointegration in clinical dentistry*. Chicago: Quintessence, 11-77. ISBN 978-0-86715-129-9.
3. Ovesy M, Voumard B, Zysset P. A nonlinear homogenized finite element analysis of the primary stability of the bone-implant interface. *Biomech Model Mechanobiol*. 2018 Oct;17(5):1471-1480. doi: 10.1007/s10237-018-1038-3. Epub 2018 Jun 1. PMID: 29858707.
4. M, Park SH, Wang HL. Methods used to assess implant stability: current status. *Int J Oral Maxillofac Implants*. 2007 Sep-Oct;22(5):743-54. PMID: 17974108.
5. Tettamanti L, Andrisani C, Bassi MA, Vinci R, Silvestre-Rangil J, Tagliabue A. Immediate loading implants: review of the critical aspects. *Oral Implantol (Rome)*. 2017 Sep 27;10(2):129-139. doi: 10.11138/orl/2017.10.2.129. PMID: 29876038; PMCID: PMC5965071.
6. Trisi P, Perfetti G, Baldoni E, Berardi D, Colagiovanni M, Scogna G. Implant micromotion is related to peak insertion torque and bone density. *Clin Oral Implants Res*. 2009;20(5):467–71.
7. Karl M, Irastorza-Landa A. Does implant design affect primary stability in extraction sites? *Quintessence Int*. 2017;48(3):219-224. doi: 10.3290/j.qi.a37690. PMID: 28168242.
8. Vantaggiato G, Iezzi G, Fiera E, Perrotti V, Piattelli A. Histologic and histomorphometric report of three immediately loaded screw implants retrieved from man after a three-year loading period. *Implant Dent*. 2008 Jun;17(2):192-9. doi: 10.1097/ID.0b013e318166d654. PMID: 18545051.
9. Di Stefano DA, Arosio P, Perrotti V, Iezzi G, Scarano A, Piattelli A. Correlation between Implant Geometry, Bone Density, and the Insertion Torque/Depth Integral: A Study on Bovine Ribs. *Dent J (Basel)*. 2019 Mar 5;7(1):25. doi: 10.3390/dj7010025. PMID: 30841588; PMCID: PMC6473399.
10. Sugiura T, Yamamoto K, Horita S, Murakami K, Kirita T. Micromotion analysis of different implant configuration, bone density, and crestal cortical bone thickness in immediately loaded mandibular full-arch implant restorations: A nonlinear finite element

- study. *Clin Implant Dent Relat Res*. 2018 Feb;20(1):43-49. doi: 10.1111/cid.12573. Epub 2017 Dec 6. PMID: 29214714.
11. Sugiura T, Yamamoto K, Horita S, Murakami K, Kirita T. Micromotion analysis of different implant configuration, bone density, and crestal cortical bone thickness in immediately loaded mandibular full-arch implant restorations: A nonlinear finite element study. *Clin Implant Dent Relat Res*. 2018 Feb;20(1):43-49. doi: 10.1111/cid.12573. Epub 2017 Dec 6. PMID: 29214714.
 12. Szmukler-Moncler S, Salama H, Reingewirtz Y, Dubruille JH. Timing of loading and effect of micromotion on bone-dental implant interface: review of experimental literature. *J Biomed Mater Res*. 1998;43(2):192–203.
 13. Kheur MG, Sandhu R, Kheur S, Le B, Lakha T. Reliability of Resonance Frequency Analysis as an Indicator of Implant Micromotion: An in Vitro Study. *Implant Dent*. 2016;25(6):783–8.
 14. Trisi P, De Benedittis S, Perfetti G, Berardi D. Primary stability, insertion torque and bone density of cylindrical implant ad modum Branemark: Is there a relationship? An in vitro study. *Clin Oral Implants Res*. 2011;22(5):567–70.
 15. Heinemann F, Hasan I, Bourauel C, Biffar R, Mundt T. Bone stability around dental implants: Treatment related factors. *Ann Anat*. 2015 May; 199:3-8. doi: 10.1016/j.aanat.2015.02.004. Epub 2015 Feb 24. PMID: 25770887
 16. Lekholm U, Zarb G. Patient selection and preparation. In: Brånemark P-I, Zarb GA, Albrektsson T (eds). *Tissue-Integrated Prostheses: Osseointegration in Clinical Dentistry*. Chicago: Quintessence, 1985:199–209
 17. Misch CE. Density of bone: effect on treatment plans, surgical approach, healing, and progressive bone loading. *Int J Oral Implantol*. 1990;6(2):23-31. PMID: 2073394.
 18. Kong L, Gu Z, Li T, Wu J, Hu K, Liu Y, Zhou H, Liu B. Biomechanical optimization of implant diameter and length for immediate loading: a nonlinear finite element analysis. *Int J Prosthodont*. 2009 Nov-Dec;22(6):607-15. PMID: 19918598.
 19. Oliscovicz NF, Shimano AC, Junior EM, Lepri CP, Cândido A. Effect of implant design and bone density in primary stability, *Braz J Oral Sci*. 2013;12(3):158-163
 20. Andrés-García R, Vives NG, Climent FH, Palacín AF, Santos VR, Climent MH, Bullón P. In vitro evaluation of the influence of the cortical bone on the primary stability of two implant systems. *Med Oral Patol Oral Cir Bucal*. 2009 Feb 1;14(2): E93-7. PMID: 19179957.
 21. Guljé FL, Meijer HJA, Abrahamsson I, Barwacz CA, Chen S, Palmer PJ, Zadeh H, Stanford CM. Comparison of 6-mm and 11-mm dental implants in the posterior region supporting fixed dental prostheses: 5-year results of an open multicenter randomized

- controlled trial. *Clin Oral Implants Res.* 2021 Jan;32(1):15-22. doi: 10.1111/clr.13674. Epub 2020 Oct 23. PMID: 33025645; PMCID: PMC7821315.
22. Trisi P, Berardi D, Paolantonio M, Spoto G, D'Addona A, Perfetti G. Primary stability, insertion torque, and bone density of conical implants with internal hexagon: Is there a relationship? *J Craniofac Surg.* 2013;24(3):841–4.
 23. Johansson C, Albrektsson T. Integration of screw implants in the rabbit: a 1-year follow-up of removal torque of titanium implants. *Int J Oral Maxillofac Implants.* 1987 Spring;2(2):69-75. PMID: 3481352.
 24. Johansson CB, Albrektsson T. a removal torque and histomorphometric study of commercially pure niobium and titanium implants in rabbit bone. *Clin Oral Implants Res* 1991 ;2:24-19.
 25. Johansson CB, Sennerby L, Albrektsston T. A removal torque and histomorphometric study of bone tissues reactions to commercially pure titanium and Vitallium implants. *Int J Oral Maxillofac Implants* 1991 ;6:437-441.
 26. Roberts WE, Smith RK, Zilberman Y, Mozsary PG, Smith RS. Osseous adaptation to continuous loading of rigid endosseous implants. *Am J Orthod* 1984;86:95-111.
 27. Lachmann S, Jäger B, Axmann D, Gomez-Roman G, Groten M, Weber H. Resonance frequency analysis and damping capacity assessment. Part I: an in vitro study on measurement reliability and a method of comparison in the determination of primary dental implant stability. *Clin Oral Implants Res.* 2006 Feb;17(1):75-9. doi: 10.1111/j.1600-0501.2005.01173.x. PMID: 16441787.
 28. McCormick, N. & Lord, J. (2010) Digital Image Correlation. *Materials Today*, 52-54.
 29. Messias, A. (2018) Rehabilitation of kennedy class I patients with removable partial dentures: retrospective clinical study and biomechanical analysis of implant-assisted options. Coimbra: Faculdade de Medicina, Universidade de Coimbra, 2018.
 30. ISO 14801 Dentistry–Implants–Dynamic loading test for endosseous dental implants
 31. Farooq M, Sazonov E. Automatic Measurement of Chew Count and Chewing Rate during Food Intake. *Electronics (Basel).* 2016;5(4):62. doi: 10.3390/electronics5040062. Epub 2016 Sep 23. PMID: 29082036; PMCID: PMC5656270.
 32. Po JM, Kieser JA, Gallo LM, Tésenyi AJ, Herbison P, Farella M. Time-frequency analysis of chewing activity in the natural environment. *J Dent Res.* 2011 Oct;90(10):1206-10. doi: 10.1177/0022034511416669. Epub 2011 Aug 1. PMID: 21810620.
 33. Pommer B, Frantal S, Willer J, Posch M, Watzek G, Tepper G. Impact of dental implant length on early failure rates: a meta-analysis of observational studies. *J Clin*

- Periodontol. 2011 Sep;38(9):856-63. doi: 10.1111/j.1600-051X.2011.01750.x. Epub 2011 Jul 3. PMID: 21722154.
34. Lum LB. A biomechanical rationale for the use of short implants. *J Oral Implantol* 1991; 17:126-31.
 35. Lee JH, Frias V, Lee KW, Wright RF. Effect of implant size and shape on implant success rates: a literature review. *J Prosthet Dent*. 2005 Oct;94(4):377-81. doi: 10.1016/j.prosdent.2005.04.018. PMID: 16198176.
 36. Rodrigues, T (2013): Medição de micromovimentos em implantes endósseos pelo método de correlação de imagem digital tridimensional Coimbra: Faculdade de Medicina, Universidade de Coimbra, 2013.
 37. H H, G W, E H. The clinical significance of implant stability quotient (ISQ) measurements: A literature review. *J Oral Biol Craniofac Res*. 2020 Oct-Dec;10(4):629-638. doi: 10.1016/j.jobcr.2020.07.004. Epub 2020 Aug 14. PMID: 32983857; PMCID: PMC7494467.
 38. Hsu, J. T., Fuh, L. J., Lin, D. J., Shen, Y. W. & Huang, H. L. (2009) Bone strain and interfacial sliding analyses of platform switching and implant diameter on an immediately loaded implant: experimental and three-dimensional finite element analyses. *J Periodontol* 80, 1125-1132
 39. Messias A, Rocha S, Calha N, Neto MA, Nicolau P, Guerra F. Effect of intentional abutment disconnection on the micromovements of the implant-abutment assembly: a 3D digital image correlation analysis. *Clin Oral Implants Res* 2015.
 40. Calha N, Messias A, Guerra F, Martinho B, Neto MA, Nicolau P. Effect of geometry on deformation of anterior implant-supported zirconia frameworks: An in vitro study using digital image correlation. *J Prosthodont Res*. 2017 Apr;61(2):139-148. doi: 10.1016/j.jpor.2016.08.004. Epub 2016 Sep 22. PMID: 27667555.
 41. Morneburg, T.R. & Proschel, P.A. (2003) In vivo forces on implants influenced by occlusal scheme and food consistency. *The International Journal of Prosthodontics*: 481–486.
 42. Serra, C.M. & Manns, A.E. (2013) Bite force measurements with hard and soft bite surfaces. *Journal of Oral Rehabilitation*: 563–568
 43. Barikani H, Rashtak S, Akbari S, Badri S, Daneshparvar N, Rokn A. The effect of implant length and diameter on the primary stability in different bone types. *J Dent (Tehran)*. 2013 Sep;10(5):449-55. Epub 2013 Sep 30. PMID: 24910653; PMCID: PMC4025419.
 44. Degidi M, Daprile G, Piattelli A. Primary stability determination by means of insertion torque and RFA in a sample of 4,135 implants. *Clin Implant Dent Relat Res*. 2012

Aug;14(4):501-7. doi: 10.1111/j.1708-8208.2010.00302.x. Epub 2010 Sep 17. PMID: 20849539.

45. Weerapong K, Sirimongkolwattana S, Sastraruji T, Khongkhunthian P. Comparative study of immediate loading on short dental implants and conventional dental implants in the posterior mandible: A randomized clinical trial. *Int J Oral Maxillofac Implants*. 2019 January/February;34(1):141–149. doi: 10.11607/jomi.6732. Epub 2018 Dec 5. PMID: 30521662.
46. Desai SR, Singh R, Karthikeyan I. 2D FEA of evaluation of micromovements and stresses at bone-implant interface in immediately loaded tapered implants in the posterior maxilla. *J Indian Soc Periodontol*. 2013 Sep;17(5):637-43. doi: 10.4103/0972-124X.119283. PMID: 24174759; PMCID: PMC3808020.

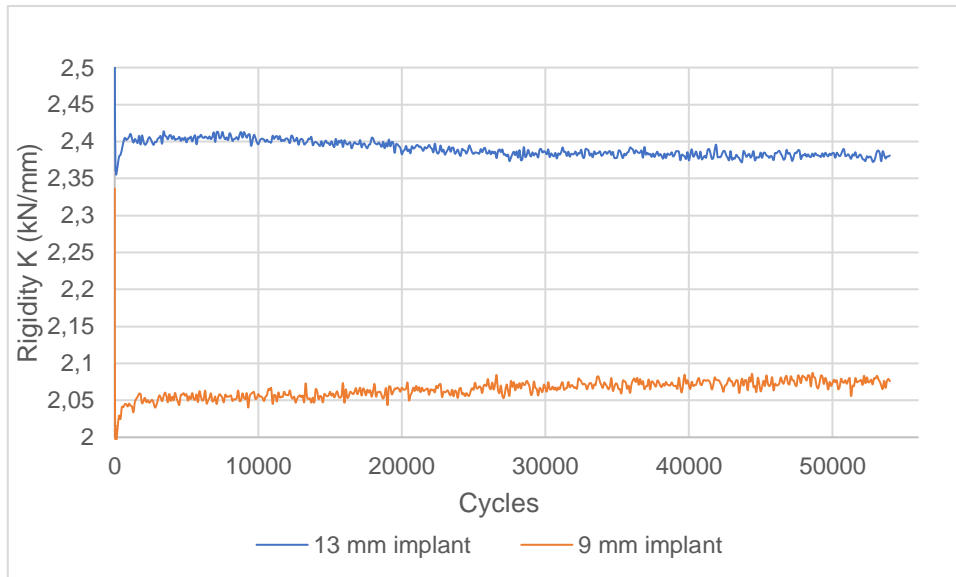
47. Appendices



Appendix I – Implant site preparation



Appendix II – Geometric support 3D design



Appendix III – Rigidity variation of the system implant-bone along the loading period